Supplemental Information

Fasting activates Fatty Acid Oxidation to enhance intestinal stem cell function during homeostasis and aging

Maria M. Mihaylova[1,2,3,9,10], Chia-Wei Cheng[2,10], Amanda Q. Cao[1,2,3,9,11], Surya Tripathi[2,11], Miyeko D. Mana[2], Khristian E. Bauer-Rowe[2], Monther Abu-Remaileh[1,2,3,9], Laura Clavain[1], Aysegul Erdemir[2], Caroline A. Lewis[1], Elizaveta Freinkman[1], Audrey S. Dickey[4], Albert R. La Spada[4], Yanmei Huang[1], George W. Bell[1], Vikram Deshpande[5], Peter Carmeliet[6,7], Pekka Katajisto[8], David M. Sabatini[1,2,3,9,12 *] and Ömer H. Yilmaz[2,3,5,12,13*]

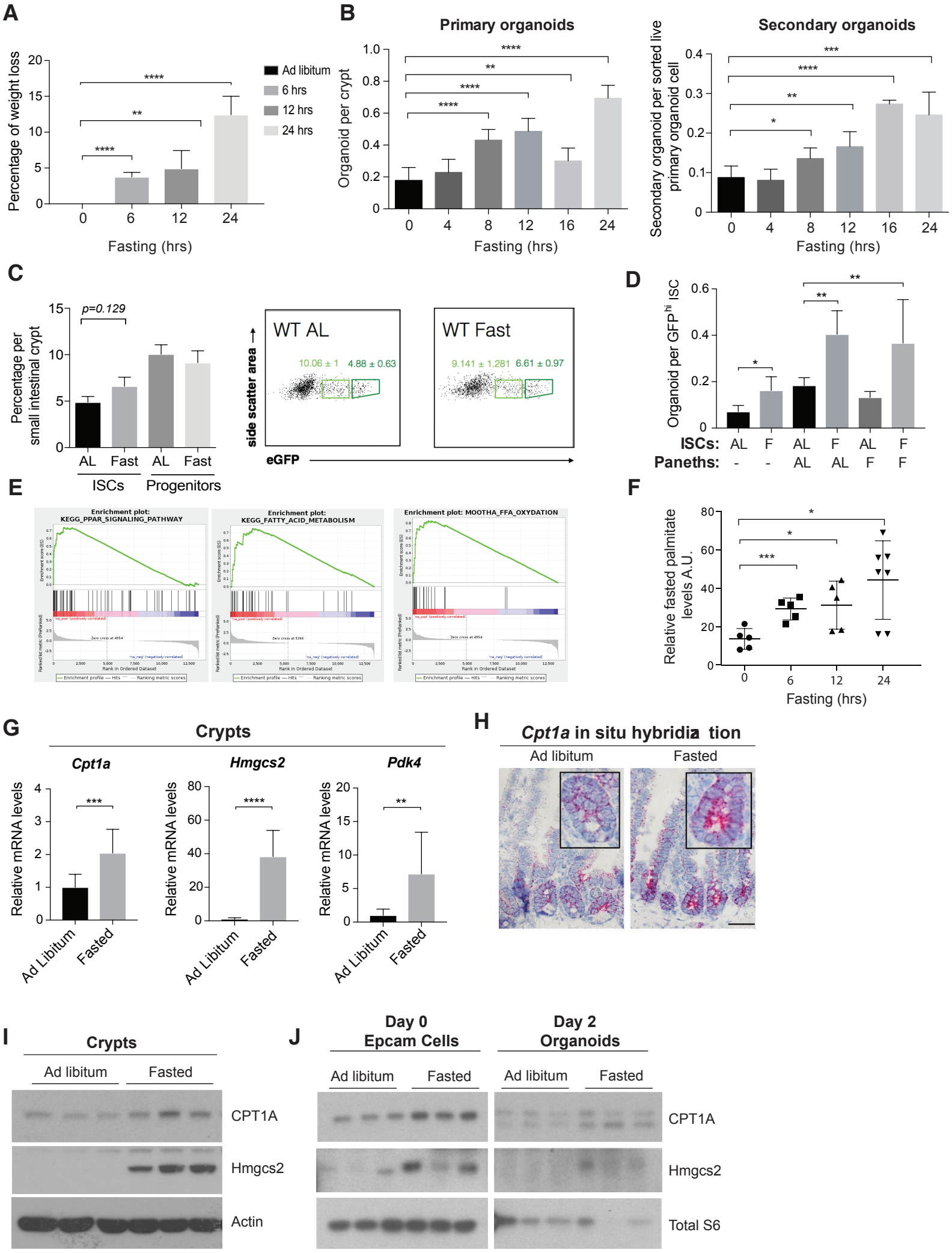
A
Percentage of weight loss
Ad libitum
6 hrs
12 hrs
24 hrs
Fasting (hrs)
B
Primary organoids
Organoid per crypt
Fasting (hrs)
Secondary organoids
Secondary organoid per sorted live primary organoid cell
Fasting (hrs)
C
Percentage per small intestinal crypt
p=0.129
AL
Fast
AL
Fast
ISCs
Progenitors
WT AL
10.06 ± 1
4.88 ± 0.63
WT Fast
9.141 ± 1.281
6.61 ± 0.97
side scatter area
eGFP
D
Organoid per GFP^hi ISC
ISCs: AL F AL F AL F
Paneths: - - AL AL F F
E
Enrichment plot: KEGG_PPAR_SIGNALING_PATHWAY
Enrichment plot: KEGG_FATTY_ACID_METABOLISM
Enrichment plot: MOOTHA_FFA_OXYDATION
Rank in Ordered Dataset
Enrichment profile
Hits
Ranking metric scores
F
Relative fasted palmitate levels A.U.
Fasting (hrs)
G
Crypts
Cpt1a
Hmgcs2
Pdk4
Relative mRNA levels
Ad Libitum
Fasted
H
Cpt1a in situ hybridia tion
Ad libitum
Fasted
I
Crypts
Ad libitum
Fasted
CPT1A
Hmgcs2
Actin
J
Day 0 Epcam Cells
Day 2 Organoids
Ad libitum
Fasted
Ad libitum
Fasted
CPT1A
Hmgcs2
Total S6

Supplementary Figure 1: Fasting induces fatty acid oxidation (FAO) and improves organoid formation of crypts and ISCs, Related to Figure 1.

(A) Weight-loss (%) during fasting. Mice were fasted for 6-24 hours and individual weight loss was measured and normalized to the original weight (ad libitum). n=5 mice per group per time point.

(B) Increased clonogenic potential in primary and secondary organoids correlated with duration of fast. n=2 mice for each time point.

(C) Quantification of ISCs (Lgr5-GFP^{hi}) and progenitor cells (Lgr5-GFP^{low}) from ad libitum (AL) and fasted animals by flow cytometry. Representative flow cytometry plots are illustrated. AL n=15, Fast n= 10.

(D) ISCs from fasted animals (F) had significantly enhanced organoid-forming capacity when mixed with aged matched AL Paneth cells. Fasted Paneth cell did not further boost clonogenic potential of ISCs. Mice were fasted for 24 hours prior to crypt isolation and cell sorting. n=3 mice per group.

(E) Gene-set enrichment analysis (GSEA) of RNA-Seq indicates fasting up-regulated PPAR targets (left), fatty acid metabolism (middle) and fatty acid oxidation (right).

(F) Fasting elevated plasma palmitate levels. Blood samples were collected from 3-4 month old mice fasted for 0, 6, 12 and 24 hours. Levels of palmitate in plasma were measured using LC-MS. n=5 per group per time point.

(G) Fasting increased mRNA expression levels of fatty acid transport and metabolism genes in intestinal crypts. *Cpt1a*, *Carnitine palmitoyltransferase I; Hmgcs2, hydroxymethylglutaryl CoA synthase 2; PDK4, pyruvate dehydrogenase kinase isoform 4.* n=12 for young AL, n=8 for young fasted.

(H) Fasting induced *Cpt1a* expression. Representative images of *Cpt1a* in situ hybridization. *Cpt1a* (red) mRNA in crypts of 3-4 month fed ad libitum or fasted for 24 hours (Fast). Scale bar, 100 μm.

(I) Western blot analysis of *Cpt1a* and *Hmgcs2* in intestinal crypts of ad libitum and fasted mice, n=3 per group.

(J) Western blots showing induced PPAR targets CPT1a and Hmgcs2 in fasted animals from sorted epithelial cells ($Epcam^{+}$) on day of plating (day 0) and retained induction in fasted organoids following post 2 days of culture in crypt/organoid media. n=3 mice each.

Unless otherwise specified, data are mean ± s.d. *$p < 0.05$, **$p < 0.01$, ***$p < 0.001$. Student's t-test, unpaired.

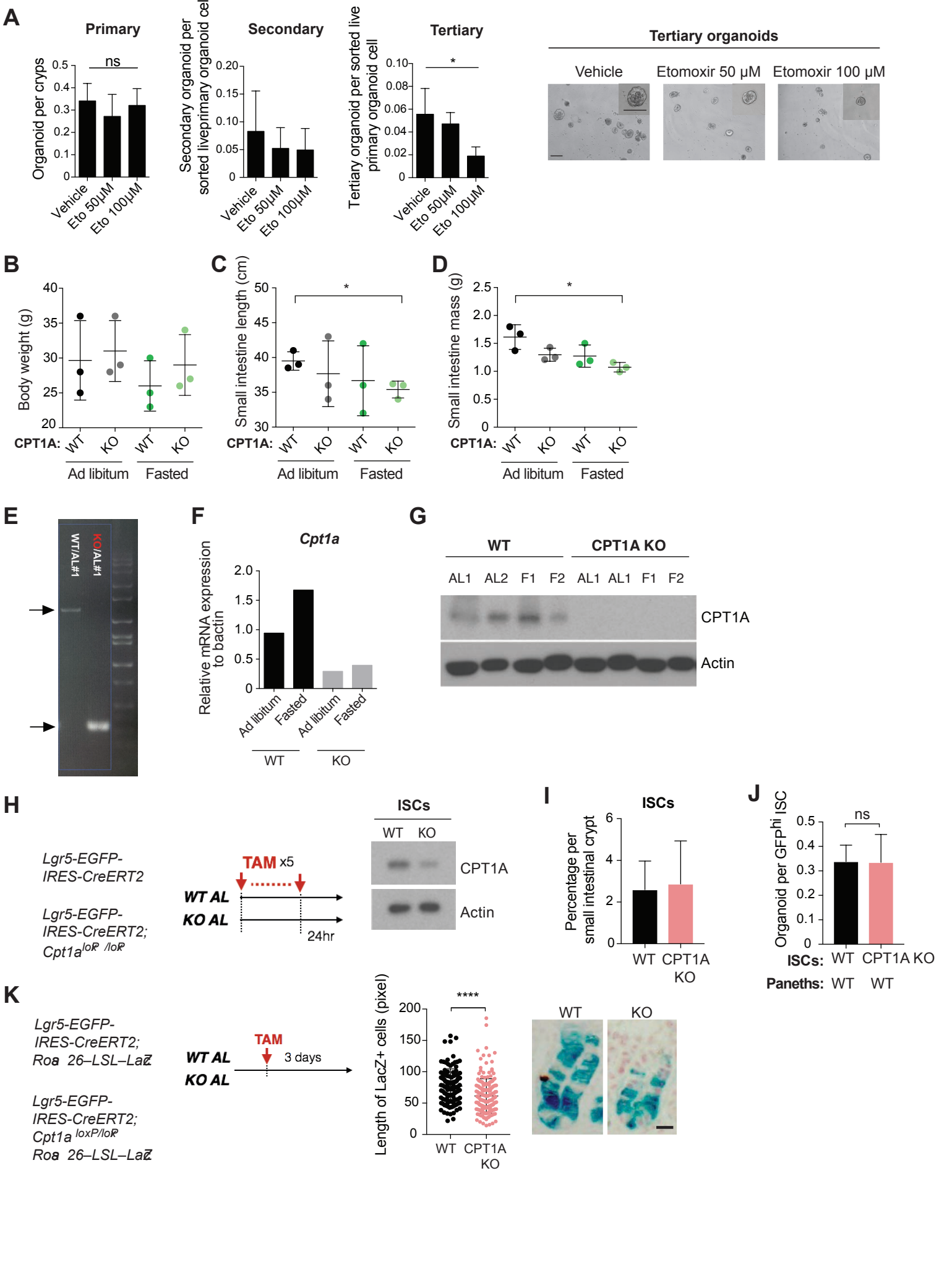
A
Primary
Organoid per cryps
ns
Vehicle
Eto 50μM
Eto 100μM
Secondary
Secondary organoid per sorted liveprimary organoid cell
Tertiary
Tertiary organoid per sorted live primary organoid cell
*
Tertiary organoids
Vehicle
Etomoxir 50 μM
Etomoxir 100 μM
B
Body weight (g)
CPT1A:
WT
KO
Ad libitum
Fasted
C
Small intestine length (cm)
D
Small intestine mass (g)
E
WT/AL#1
KO/AL#1
F
Cpt1a
Relative mRNA expression to bactin
WT
KO
G
WT
CPT1A KO
AL1
AL2
F1
F2
CPT1A
Actin
H
Lgr5-EGFP-IRES-CreERT2
Lgr5-EGFP-IRES-CreERT2; Cpt1a loxP /loxP
TAM x5
WT AL
KO AL
24hr
ISCs
I
Percentage per small intestinal crypt
J
Organoid per GFPhi ISC
ISCs:
Paneths:
K
Lgr5-EGFP-IRES-CreERT2; Rosa 26–LSL–LacZ
Lgr5-EGFP-IRES-CreERT2; Cpt1a loxP/loxP Rosa 26–LSL–LacZ
TAM
3 days
Length of LacZ+ cells (pixel)
****

Supplementary Figure 2: Inhibition of FAO impairs organoid formation ex- vivo, Related to Figure 2.

(A) Inhibition of CPT1A by etomoxir reduced tertiary organoid-forming capacity of naïve crypts derived from ad libitum mice. From left to right, frequencies of organoid formation from crypts (primary, day 3), from 5,000 sorted live primary organoid cells (secondary, day 3) and from 5,000 sorted live secondary organoid cells (tertiary day 3). n=3 per group. Scale bar, 100 μm.

(**B**) Deletion of *Cpt1a* gene did not affect body weight. n=3 mice per group.

(C- D) *Cpt1a* deletion reduced small intestinal length **(C)** and small intestinal mass (**D**) only upon fasting compared to controls. n=3 mice per group.

(E) Confirmation of *Cpt1a* deletion. Gene deletion was confirmed by PCR using the outside primers framing the loxp sites.

(F) Confirmation of disrupted *Cpt1a* mRNA by qRT-PCR relative to b-actin levels in KO mice versus controls in ad libitum and fasted states.

(G) Confirmation of CPT1A protein depletion in intestinal crypts of CPT1A KO mice compared to controls.

(H) Schematic of acute ablation of CPT1A in ISCs in the *Lgr5-EGFP-IRES-CreERT2* model and western blot analysis from sorted ISCs showing CPT1A depletion versus control levels.

(**I**) Quantification of GFP^+ ISCs in *Lgr5-EGFP-CreERT2* and *Lgr5-EGFP-CreERT2; Cpt1a* $^{lox/lox}$ mice by flow cytometry analysis. n=3 each.

(**J**) Frequency of organoids formed per ISCs in *Lgr5-EGFP-IRES-CreERT2* and *Lgr5-EGFP-IRES-CreERT2; Cpt1a* $^{lox/lox}$ mice. WT n=4, CPT1a KO n=4

(K) Schematic of lineage tracing experiments and quantification of number of LacZ positive cells upon *Cpt1a* loss and in controls. WT n=3, CPT1a KO= 4.

Unless otherwise specified, data are mean ± s.d. **p < 0.05, ****p<0.0005*. Student's t-test, unpaired. Scale bar, 20 μm.

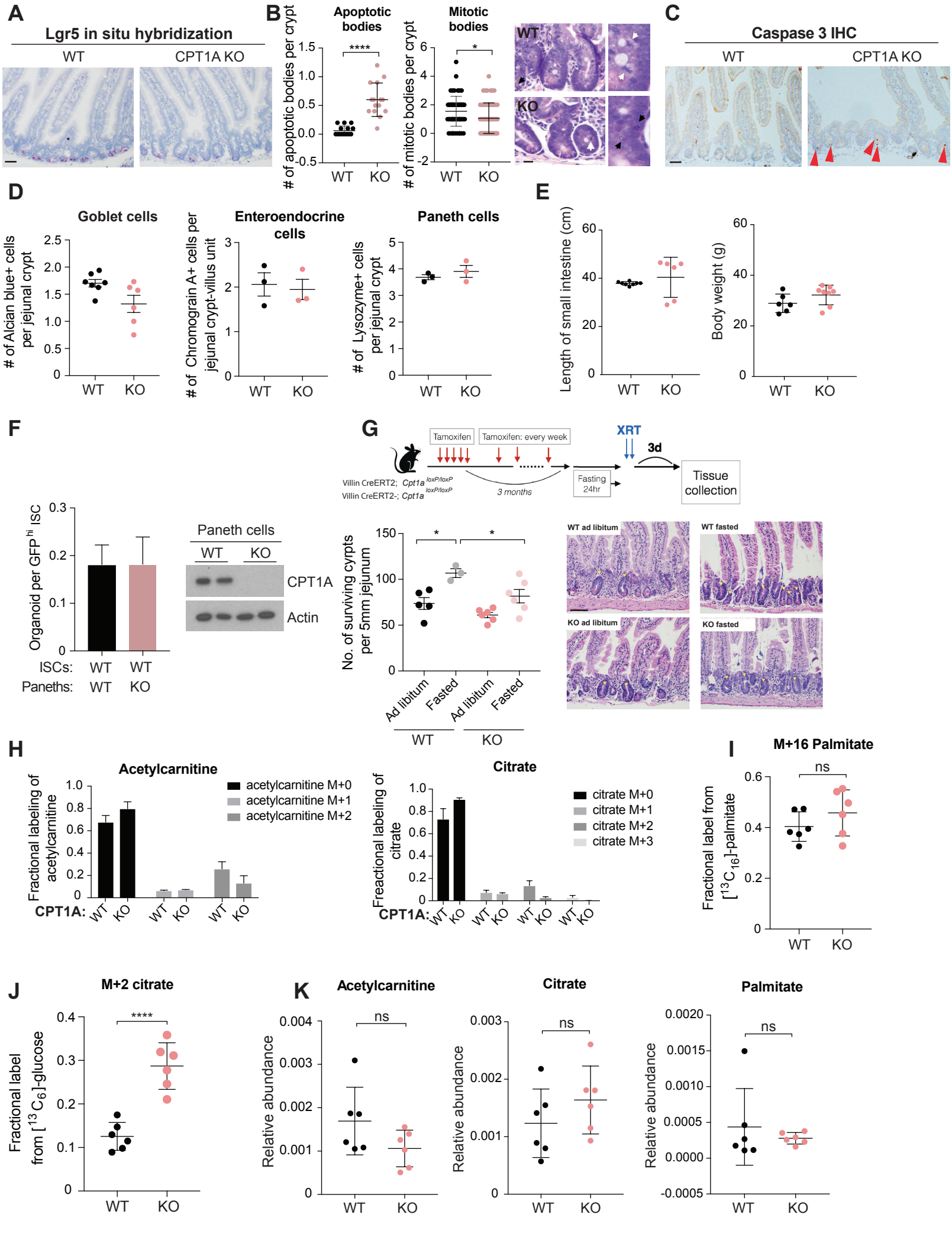
A
Lgr5 in situ hybridization
WT
CPT1A KO
B
Apoptotic bodies
# of apoptotic bodies per crypt
****
WT
KO
Mitotic bodies
# of mitotic bodies per crypt
*
WT
KO
C
Caspase 3 IHC
WT
CPT1A KO
D
Goblet cells
# of Alcian blue+ cells per jejunal crypt
Enteroendocrine cells
# of Chromograin A+ cells per jejunal crypt-villus unit
Paneth cells
# of Lysozyme+ cells per jejunal crypt
E
Length of small intestine (cm)
Body weight (g)
F
Organoid per GFP^hi ISC
ISCs: WT WT
Paneths: WT KO
Paneth cells
WT
KO
CPT1A
Actin
G
Tamoxifen
Tamoxifen: every week
XRT
3d
Villin CreERT2; Cpt1a loxP/loxP
Villin CreERT2-; Cpt1a loxP/loxP
3 months
Fasting 24hr
Tissue collection
No. of surviving crypts per 5mm jejunum
Ad libitum
Fasted
WT
KO
WT ad libitum
WT fasted
KO ad libitum
KO fasted
H
Acetylcarnitine
Fractional labeling of acetylcarnitine
acetylcarnitine M+0
acetylcarnitine M+1
acetylcarnitine M+2
CPT1A:
Citrate
Freactional labeling of citrate
citrate M+0
citrate M+1
citrate M+2
citrate M+3
I
M+16 Palmitate
ns
Fractional label from [13C16]-palmitate
J
M+2 citrate
****
Fractional label from [13C6]-glucose
K
Acetylcarnitine
Citrate
Palmitate
ns
Relative abundance

Supplementary Figure 3: Long-term CPT1A deletion reduces ISC numbers and proliferation, Related to Figure 3.

(A) Representative images of *in situ* hybridization for *Lgr5* levels in *Villin-CreERT2*$^{-}$; *Cpt1a*$^{loxP/loxP}$ and *Villin-CreERT2*; *Cpt1a*$^{loxP/loxP}$ intestines. n= 3 mice per group. Scale bar, 100 μm.

(B) Long-term intestinal deletion of CPT1A increased apoptosis and reduced mitosis in intestinal crypts. Representative images indicate apoptotic bodies (black arrowhead) and mitotic bodies (white arrowhead) in intestinal crypts of WT and CPT1A KO mice. n= 3 mice per group. Scale bar, 20 μm.

(C) CPT1A KO intestines have significantly higher Caspase 3 positive cells in crypts compared to controls. Immunostains for Caspase 3 positive cells in WT and CPT1A KO intestines. Arrows represent Caspase 3 positive cells in the crypts. n= 3 mice per group. Scale bar, 100 μm.

(D) Enumeration of goblet, enteroendocrine and Paneth cells showed no differences between CPT1A KO intestines compared to WT. n= 3 mice per group.

(E) Body weight and intestinal length of WT and CPT1A KO intestines remained unchanged. n=6 mice per group.

(F) Mixing experiment of WT ISCs with WT or CPT1A KO Paneth cells. n=4 mice WT and n=4 mice CPT1A KO mice. Adjacent panel is western blot analysis confirming CPT1a deletion.

(G) Quantification of surviving crypts from WT ad libitum, WT fasted, CPT1A KO ad libitum and CPT1A KO fasted irradiated mice. WT Ad libitum n=5, WT Fasted n=3, CPT1A KO Ad libitum n= 6, CPT1A KO Fasted n=6. Scale bar, 100 μm.

(H) Fraction of total levels of acetylcarnitine and citrate for WT and CPT1A KO crypts labeled with [U-^{13}C] palmitate. n=6 WT and n=6 CPT1A KO mice.

(I) Fraction of total levels of M+16 palmitate for WT and CPT1A KO crypts labeled with [U^{13}-C] palmitate. n=6 WT and n=6 CPT1A KO mice.

(J) Fractional labeling of M+2 citrate following [U-^{13}C] glucose tracing. n=6 WT and n=6 CPT1A KO mice. n=6 WT and n=6 CPT1A KO mice.

(K) Total pools normalized to total protein for acetylcarnitine, citrate and palmitate. n=6 WT and n=6 CPT1A KO mice. n=6 WT and n=6 CPT1A KO mice.

Unless otherwise specified, data are mean ± s.d. *$p < 0.05$, **$p < 0.01$, ***$p < 0.001$, ****$p<0.0005$. Student's t-test, unpaired.

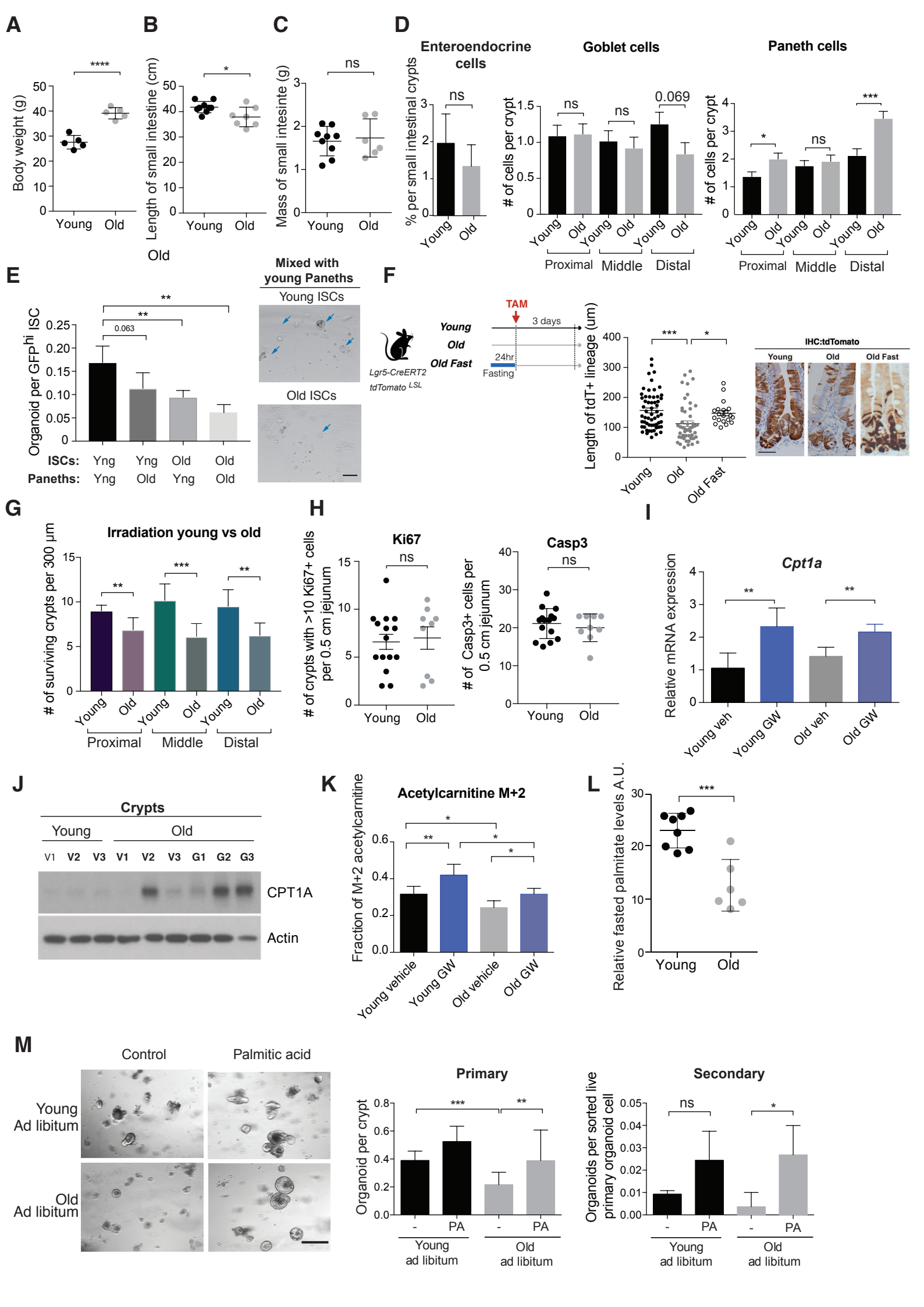
A
B
C
D
Body weight (g)
Length of small intestine (cm)
Mass of small intesinte (g)
Young
Old
****
*
ns
Enteroendocrine cells
Goblet cells
Paneth cells
% per small intestinal crypts
# of cells per crypt
0.069
***
Proximal
Middle
Distal
E
Mixed with young Paneths
Young ISCs
Old ISCs
Organoid per GFP^hi ISC
0.063
ISCs: Yng Yng Old Old
Paneths: Yng Old Yng Old
F
TAM
3 days
24hr
Fasting
Young
Old
Old Fast
Lgr5-CreERT2
tdTomato LSL
Length of tdT+ lineage (um)
IHC:tdTomato
G
Irradiation young vs old
# of surviving crypts per 300 µm
H
Ki67
# of crypts with >10 Ki67+ cells per 0.5 cm jejunum
Casp3
# of Casp3+ cells per 0.5 cm jejunum
I
Cpt1a
Relative mRNA expression
Young veh
Young GW
Old veh
Old GW
J
Crypts
V1 V2 V3 V1 V2 V3 G1 G2 G3
CPT1A
Actin
K
Acetylcarnitine M+2
Fraction of M+2 acetylcarnitine
Young vehicle
Young GW
Old vehicle
Old GW
L
Relative fasted palmitate levels A.U.
M
Control
Palmitic acid
Young Ad libitum
Old Ad libitum
Primary
Secondary
Organoid per crypt
Organoids per sorted live primary organoid cell
PA
Young ad libitum
Old ad libitum

Supplementary Figure 4: Age-associated decline of intestinal stem cell numbers and function, Related to Figure 4.

(A) Aging significantly increased body mass. young: n=5, old: n=5.

(B) In comparison to young mice, old mice had shorter small intestines young: n=10, old: n=7).

(C) Aging did not change small intestinal mass. young: n=8, old: n=7.

(D) No significant difference in the numbers of enteroendocrine cells and goblet cells, while region specific increase of Paneth cells was detected in crypts of old mice relative to young mice. young: n=6, old: n=7.

(E) Aged stem cells have reduced capacity for organoid formation. Mixing experiment of young and old ISCs with young and old Paneth cells. Counts performed at day 3 post plating. n=4 per group. Scale bar, 20 μm.

(F) Enhanced intestinal stem cell function following fasting in aged animals. Lgr5-derived tdTomato^{+} (tdT^{+}) progeny were significantly reduced during aging. Representative pictures of tdT^{+} Lgr5-derived progeny in the proximal intestine in young and aged Lgr5-cre;tdTomato^{LSL} mice, at 3 days post one tamoxifen injection. Scale bar, 50 μm.

(G) Intestinal crypts from aged animal were compromised after challenged by a lethal dose of irradiation (7.5Gy x 2). Numbers of surviving crypts per 300 μm in the indicated region (i.e. proximal, middle and distal small intestine) after ionizing irradiation-induced (XRT) damage in young and aged mice. n=6 to 8 per group.

(H) Quantification of ki67 and Casp3 positive cells in animals described in (**G)**.

(I) qRT-PCR analysis for *Cpt1a* mRNA levels in sorted ISCs from vehicle (veh) or GW501516 (GW) treatment group, n=6 per group.

(J) Western blot analysis of protein levels of CPT1A in crypts from young or old mice treated with vehicle or GW501516 (GW); Young vehicle (V) n = 3, Old vehicle (V) n= 3, GW (G) n=3 per group.

(K) Results of [U-^{13}C] palmate labeling experiment indicate an increase of FAO *in vivo* following GW treatment. Animals were treated with vehicle or GW for 3-4 weeks. Crypts from young vehicle and GW treated animals were labeled using [U-^{13}C] palmitate for 1 hour and analyzed using LC-MS. n=7 for young vehicle, n=5 for young GW, n=6 for old vehicle and n=3 for old GW.

(L) Levels of fasting plasma palmitate are significantly lower in old mice. Blood samples were collected from young and old mice fasted for 24 hours. Levels of palmitate in plasma were measured using LC-MS. Young n=8, old n=6 per group per time point.

(M) In vitro exposure to palmitic acid increases both the primary and secondary organoid potential of naive crypts from old mice fed ad libitum (AL). Representative images of day-3 organoids. Primary: Young AL, old AL and old fasted mice cultured with 30 μM palmitic acid (PA) in primary organoid cultures. Secondary: Frequencies of organoid formation from crypts (primary, day-5) and of 5,000 sorted live primary organoid cells (secondary, day-3) after 7-10 days of 30 μM palmitic acid treatment. n= 8 replicates, n=4 mice. Scale bar, 100 μm.

Unless otherwise specified, data are mean ± s.d. *$p < 0.05$, **$p < 0.01$, ***$p < 0.001$, ****$p<0.0005$. Student's t-test, unpaired.

Supplemental Table 1 (related to STAR Methods). Primer sequence:

Primer	Sequence
Beta actin F:	GGCTGTATTCCCCTCCATCG
Beta actin R:	CCAGTTGGTAACGCCATGT
Cpt1a F:	CCATGAAGCCCTCAAACAGATC
Cpt1a R:	ATCACACCCACCACCACGATA
Hmgcs2 F:	ATACCACCAACGCCTGTTATGG
Hmgcs2 R:	CAATGTCACCACAGACCACCAG
Pdk4 F:	AGGGAGGTCGAGCTGTTCTC
Pdk4 R:	GGAGTGTTCACTAAGCGGTCA